AFRL-RY-WP-TP-2013-0022

GENERATION AND MODULATION OF A MILLIMETER-WAVE SUBCARRIER ON AN OPTICAL FREQUENCY GENERATED VIA OPTICAL INJECTION (POSTPRINT)

Nicholas G. Usechak

Optoelectronic Technology Branch
Aerospace Components & Subsystems Division

Michael Pochet and Timothy Locke

Air Force Institute of Technology

JANUARY 2013
Interim

AIR FORCE RESEARCH LABORATORY
SENSORS DIRECTORATE
WRIGHT-PATTERSON AIR FORCE BASE, OH 45433-7320
AIR FORCE MATERIEL COMMAND
UNITED STATES AIR FORCE

REPORT DOCUMENTATION PAGE

Form Approved
OMB No. 0704-0188

1. REPORT DATE *(DD-MM-YY)*	2. REPORT TYPE	3. DATES COVERED *(From - To)*
January 2013	Journal Article Postprint	15 September2008 – 27 September 2012

4. TITLE AND SUBTITLE
GENERATION AND MODULATION OF A MILLIMETER-WAVE SUBCARRIER ON AN OPTICAL FREQUENCY GENERATED VIA OPTICAL INJECTION (POSTPRINT)

5a. CONTRACT NUMBER
In-house

5b. GRANT NUMBER

5c. PROGRAM ELEMENT NUMBER
61102F

6. AUTHOR(S)
Nicholas G. Usechak (AFRL/RYDH)
Michael Pochet and Timothy Locke (Air Force Institute of Technology)

5d. PROJECT NUMBER
2305

5e. TASK NUMBER
DP

5f. WORK UNIT NUMBER
Y05T

7. PERFORMING ORGANIZATION NAME(S) AND ADDRESS(ES)
Optoelectronic Technology Branch
Aerospace Components & Subsystems Division
Air Force Research Laboratory, Sensors Directorate
Wright-Patterson Air Force Base, OH 45433-7320
Air Force Materiel Command, United States Air Force

Air Force Institute of Technology

8. PERFORMING ORGANIZATION REPORT NUMBER
AFRL-RY-WP-TP-2013-0022

9. SPONSORING/MONITORING AGENCY NAME(S) AND ADDRESS(ES)
Air Force Research Laboratory
Sensors Directorate
Wright-Patterson Air Force Base, OH 45433-7320
Air Force Materiel Command
United States Air Force

10. SPONSORING/MONITORING AGENCY ACRONYM(S)
AFRL/RYDH

11. SPONSORING/MONITORING AGENCY REPORT NUMBER(S)
AFRL-RY-WP-TP-2013-0022

12. DISTRIBUTION/AVAILABILITY STATEMENT
Approved for public release; distribution unlimited.

13. SUPPLEMENTARY NOTES
Journal article published in IEEE Photonics Journal, October 2012. ©2012 IEEE. The U.S. Government is joint author of the work and has the right to use, modify, reproduce, release, perform, display or disclose the work. PAO Case Number 88ABW-2012-4420, Clearance Date 10 August 2012. Report contains color.

14. ABSTRACT
A highly tunable millimeter-wave subcarrier signal is generated by optically injecting a Fabry–Perot semiconductor laser. The optically injected light, which enables microwave subcarrier frequencies well beyond the injected laser's free-running relaxation oscillation frequency, is then on–off keyed by direct-current (dc) modulation of the injected slave laser. Adjustment of the subcarrier frequency is easily accomplished by changing either the dc bias current and/or junction temperature of the injected slave or the injecting master laser. In this paper, we theoretically and experimentally investigate the purity of the modulated microwave subcarrier. The generated microwave signal was then transmitted over 50 km of single-mode fiber, demonstrating the applicability of a directly modulated slave laser optically injected into the period-one state for radio-over-fiber applications.

15. SUBJECT TERMS
Microwave Photonics, Semiconductor Lasers, Injection-Locked Lasers sources

16. SECURITY CLASSIFICATION OF:			17. LIMITATION OF ABSTRACT:	18. NUMBER OF PAGES	19a. NAME OF RESPONSIBLE PERSON (Monitor)
a. REPORT	b. ABSTRACT	c. THIS PAGE			Nicholas Usechak
Unclassified	Unclassified	Unclassified	SAR	14	19b. TELEPHONE NUMBER *(Include Area Code)* N/A

IEEE Photonics Journal
An IEEE Photonics Society Publication

Open Access

Generation and Modulation of a Millimeter-Wave Subcarrier on an Optical Frequency Generated via Optical Injection

Volume 4, Number 5, October 2012

Michael Pochet
Timothy Locke
N. G. Usechak

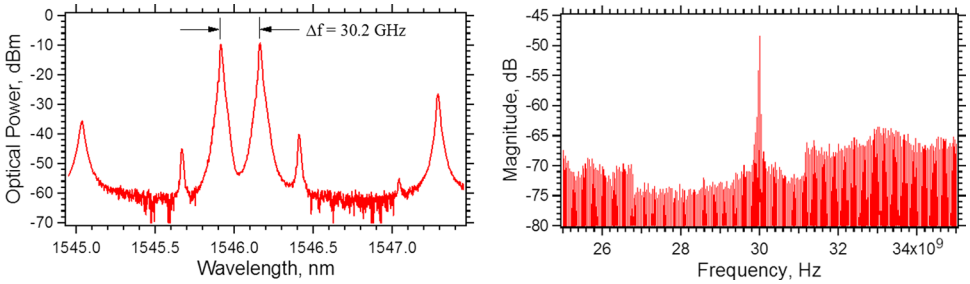

DOI: 10.1109/JPHOT.2012.2219042
1943-0655/$31.00 ©2012 IEEE

Generation and Modulation of a Millimeter-Wave Subcarrier on an Optical Frequency Generated via Optical Injection

Michael Pochet,[1] Timothy Locke,[1] and N. G. Usechak[2]

[1]U.S. Air Force Institute of Technology WPAFB, OH 45433 USA
[2]U.S. Air Force Research Laboratory, WPAFB, OH 45433 USA

DOI: 10.1109/JPHOT.2012.2219042
1943-0655/$31.00 ©2012 IEEE

Manuscript received August 17, 2012; revised September 11, 2012; accepted September 11, 2012. Date of current version September 27, 2012. The work of N. Usechak was supported by the Air Force Office of Scientific Research. Corresponding author: M. Pochet (e-mail: michael.pochet@afit.edu).

Abstract: A highly tunable millimeter-wave subcarrier signal is generated by optically injecting a Fabry–Perot semiconductor laser. The optically injected light, which enables microwave subcarrier frequencies well beyond the injected laser's free-running relaxation-oscillation frequency, is then on–off keyed by direct-current (dc) modulation of the injected slave laser. Adjustment of the subcarrier frequency is easily accomplished by changing either the dc bias current and/or junction temperature of the injected slave or the injecting master laser. In this paper, we theoretically and experimentally investigate the purity of the modulated microwave subcarrier. The generated microwave signal was then transmitted over 50 km of single-mode fiber, demonstrating the applicability of a directly modulated slave laser optically injected into the period-one state for radio-over-fiber applications.

Index Terms: Microwave photonics, semiconductor lasers.

1. Introduction

Photonic methods for generating millimeter-wave (mm-wave) signals have attracted substantial interest in the communities of radio-over-fiber (ROF) networks, broadband wireless access networks, sensor applications, radar, and satellite communications. During the past several years, multiple methods and architectures have emerged to efficiently enable the photonic generation of mm-wave signals and can be classified into various categories: dual-wavelength laser sources [1], [2]; generation using external modulation [3]–[5]; optical phase-locked-loop methods [6]; mode-locked lasers [7], [8]; and optical injection using semiconductor lasers [9]–[12]. Particular attention has been given to ROF technology, whereby optical fiber links are used to distribute mm-wave signals from a central location to remote antenna units. Interest has recently grown in ROF because it is seen as a possible solution to alleviate the frequency congestion and bit-rate limitations that are inherent in current wireless systems [13], [14]. Among the approaches for generating and modulating mm-wave signals on an optical carrier, the most straightforward technique involves a directly modulated laser for baseband transmission followed by an external modulator for optical mm-wave generation [5]. The drawbacks to schemes, which rely on external modulators, include their requirement for a precision high-speed electrical oscillator operating at the mm-wave subcarrier frequency, an RF amplifier and any other RF components to drive the modulator, and precision high-speed modulators themselves. All of these components serve to increase the cost and complexity of the system.

In this paper, external optical injection of a directly modulated Fabry–Perot semiconductor laser is investigated theoretically and experimentally. The external optical injection approach utilizes the so-called period-one state, which can be obtained in isolated regions of injected optical power/carrier frequency space. Here, it should be noted that the period-one state enables subcarrier frequency generation well beyond the electrical and free-running frequency response of the injected laser [15]–[20]. Moreover, the external optical injection scheme eliminates the need for an external modulator, an RF amplifier, or an electrical oscillator, which would otherwise be needed for the generation of the mm-wave optical subcarrier.

The applicability of using the period-one state for all-optical amplitude-modulation to frequency-modulation conversion has been previously demonstrated whereby the externally injected light is amplitude modulated resulting in the modulation of the period-one frequency [21]. Another work has investigated approaches to using the period-one state for mm-wave generation but required a double locking approach whereby the modulated laser is injected into the period-one state and electronically modulated at the mm-wave subcarrier frequency being generated to improve the stability of the signal [22]. Other relevant research reported on the high degree of tunability of the mm-wave signal, from roughly the relaxation-oscillation frequency of the slave laser to $7\times$ this value [23]. In addition to these experimental findings, a vast amount of research has investigated numerical techniques for determining the stability properties of semiconductor lasers subject to external injection [24]–[28].

This paper focuses on using the period-one state for direct generation of a microwave subcarrier signal that is broadly tunable and capable of gigabit-per-second data rates. A notable benefit of the approach employed in this paper is that microwave signals can be generated at frequencies that exceed the electronic capabilities of the injected laser, due to parasitic effects of the device and its packaging, by a factor of seven or more. Here, the electronic modulation capability of the directly modulated laser limits the maximum achievable data rate, as the microwave subcarrier signal is generated all optically. The experimental results reported in this paper are limited to the microwave range due to the experimental configuration; however, the generation of mm-wave subcarrier frequencies well beyond 30 GHz are possible. Thus, the injected optical power effect on the device is to enhance and undamp the resonance frequency of the injected slave laser, well beyond its free-running relaxation-oscillation frequency.

In addition to demonstrating the direct generation and modulation concept experimentally, this paper compares these experimental findings to a single-mode rate equation model. This model, which describes the operation of an optically injected semiconductor laser under current modulation, is solved numerically and found to agree with the experimental results. Moreover, by including noise terms in the driving current and injected optical power, the impact of operating noise can be investigated. The results obtained indicate that the scheme described in this paper appears to be a good candidate for the direct generation of mm-wave subcarrier signals and implementation in ROF architectures.

2. Millimeter-Wave Generation Under Optical Injection

The period-one state, used as the mechanism for mm-wave generation in this paper, describes the condition where the injected slave laser is locked to the injected master laser's field and the coupled system oscillates at the injected frequency (f_{inj}) with sidebands located at frequencies of $f_{inj} \pm f_r$, where f_r is the enhanced resonance frequency of the optically injected laser. As a consequence, the slave laser's electric field oscillates without being damped toward a steady-state value [16], [18]–[21]. This undamped steady-state oscillation is illustrated in Fig. 1, where the undamped resonance frequency of 30.2 GHz is observed. Fig. 1 also shows the electrical power spectra of the period-one subcarrier after the optical signal is input into a high-speed photodetector.

Previous work has shown that the operating state (i.e., stable locking, period one, period doubling, or chaos) of an optically injected semiconductor can be theoretically investigated via a single-mode rate equation model [25]–[28]. A basic pictorial description of the optical power spectra of the respective operational states (period doubling, period one, and stable injection locking),

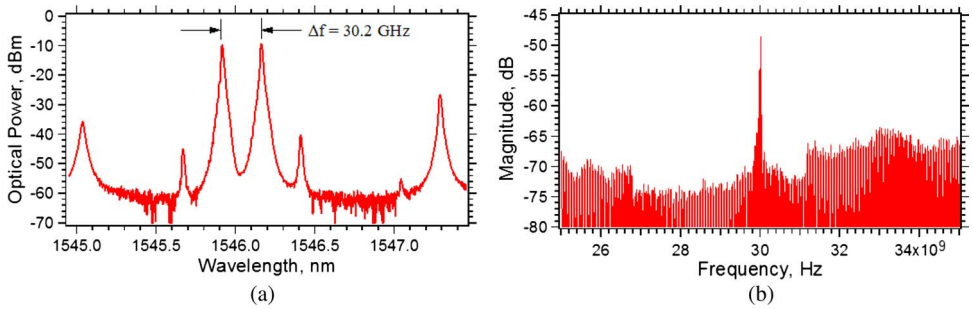

Fig. 1. (a) Optical power spectra and (b) electrical power spectra of the mm-wave subcarrier signal.

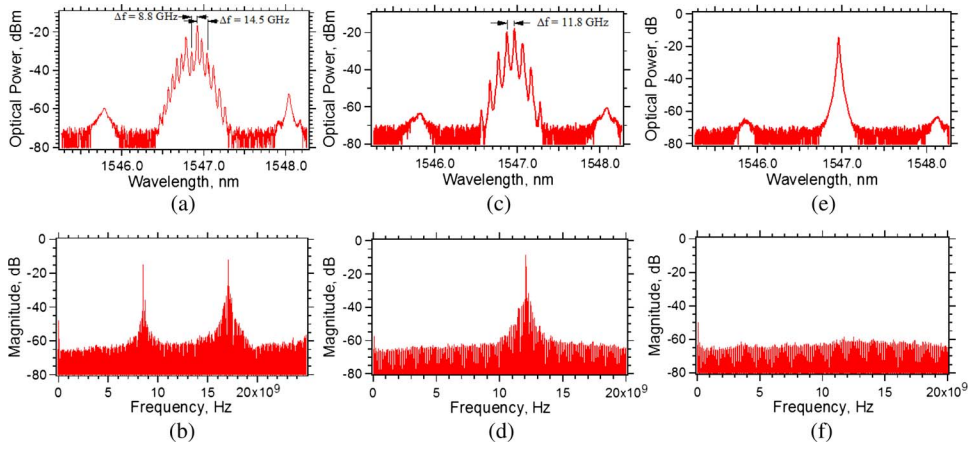

Fig. 2. (Top) Optical power spectra and (bottom) microwave power spectra of the operational states resulting from optical injection. (a) and (b) Period-doubling state where undamped resonance frequencies of 8.8-GHz (period doubling) and 14.5-GHz (period-one) are observed. (c) and (d) Period-one state where an undamped resonance frequency of 11.8-GHz is observed. (e) and (f) Stable injection locking where the resonance frequency is damped. In each, the injected master laser power was held constant while the detuning frequency was varied. For each case, the adjacent longitudinal modes of the Fabry–Perot cavity are suppressed by more than 35 dB.

collected during this investigation, is given in Fig. 2. These results are accompanied by their associated electrical power spectra. An examination of Fig. 2 reveals that the steady-state microwave frequency is correlated to the undamped resonance observed in the optical domain. When comparing the undamped resonances in the optical spectra with that observed in the electrical power spectra of the period-doubling state, as given in Fig. 2(a) and (b), the undamped resonance frequency of the period-one resonance is not correlated between the two representative spectra (14.5 GHz versus 17.1 GHz); this is attributed to instabilities in the period-doubling state and the varied data collection sweep times of the optical and electrical spectrum analyzers. In the period-one state case illustrated in Fig. 2(c) and (d), the longitudinal modes of the Fabry–Perot slave laser away from the injected mode are suppressed more than 35 dB below the carrier, enabling transmission over medium- to long-haul communication distances.

3. Modeling mm-Wave Generation and Modulation Under Optical Injection

Prior to experimental validation of the external optical-injection-based mm-wave generation approach, the 3-D system was numerically solved to determine the effect direct modulation of the slave laser's pumping current has on the combined system's output. To validate the model, the operational behavior of the optically injected laser is first evaluated using the single-mode rate equation model by solving the coupled differential equations in the time domain and qualitatively

evaluating the electric-field solution under equilibrium conditions, yielding bifurcation diagrams as described in references [27] and [28]. The mm-wave generation parameter space, identified as the region where period-one operation is observed, is then determined as a function of the injected-field ratio and detuning frequency between the master and slave lasers [23]. Given a known period-one parameter space based on the bifurcation diagrams, the modulation of the generated mm-wave is modeled by holding the simulated injection conditions constant within this region, while the operating point of the injected slave laser (bias current) is directly modulated. The direct modulation of the injected slave laser allows the coupled system to be driven into and out of the period-one state, resulting in the modulation of the mm-wave signal. The large signal modulation acts to push the laser below threshold operation in the low state, while the ON-state moves the laser bias condition above threshold, where the slave laser reaches steady state under period-one operation due to the presence of the continuous wave injected optical power.

To simulate the long-time response of the optically injected system, the normalized rate equations, given by (1)–(3), are solved, while the slave laser's electrical pumping term P is modulated

$$\frac{dY}{d\tau} = YZ + \eta_N \cos(\theta) \tag{1}$$

$$\frac{d\theta}{d\tau} = -\Omega + \alpha Z - \frac{\eta_N}{Y}\sin(\theta) \tag{2}$$

$$T\frac{dZ}{d\tau} = P - Z - (1+2Z)Y^2. \tag{3}$$

In (1)–(3), Y describes the amplitude of the electric field, θ is the phase difference between the electric fields of the master and slave lasers, and Z is the carrier density above threshold [29]. The time τ is normalized to the photon lifetime $(\tau = t/\tau_p)$. The model is dependent on three parameters derived from the free-running slave laser: T, P, and α [29]. $T = (\gamma_c/\gamma_s)$, where γ_c is the cavity decay rate and γ_s is the spontaneous carrier relaxation rate. γ_s and γ_c are independent of the slave laser's output power or the injected photon density, making T constant regardless of the bias current applied to the slave laser. P is proportional to the pumping current above threshold and is calculated using $P = (1/2)(\gamma_n/\gamma_s) \propto (J - J_{th})/J_{th}$, where J_{th} is the threshold current density. γ_n is the free-running differential carrier relaxation rate and is dependent on the laser's bias current. α is the linewidth-enhancement factor of the injected slave laser. η_N is the normalized injection strength, and Ω is the detuning parameter normalized to the cavity decay rate given $\Omega = \Delta f/\gamma_c$. The free-running relaxation-oscillation frequency (Ω_{fr}) and damping rate (γ_{fr}), normalized to the cavity decay rate, are given in (4) and (5). The unnormalized free-running relation oscillation frequency (Ω_{fr}) and damping rate (γ_{fr}) are related to $\gamma_n, \gamma_c, \gamma_s$ given the simplified relationship where the impact of the nonlinear carrier relation rate is ignored: $\Omega_{fr} = \gamma_n\gamma_c$ and $\gamma_{fr} = \gamma_n + \gamma_s$

$$\Omega_{fr} \cong \sqrt{\frac{2P}{T}} \tag{4}$$

$$\gamma_{fr} \cong \frac{(1+2P)}{2T}. \tag{5}$$

By experimentally characterizing the free-running operation of the slave laser using either the modulation bandwidth response (S21) or the ringing observed in the transient temporal response of the device when subjected to pulsed modulation, the parameters P and T can be determined via (4) and (5). In this paper, the linewidth-enhancement factor of the slave laser was measured using the injection-locking approach described in [30].

The simulated temporal response of the slave-laser-modulated system is given in Fig. 3, where the injected field ratio (η_N) and detuning frequency (Ω) are held constant, while the pumping term P is modulated using a pseudorandom bit sequence (PRBS). Specifically, the PRBS used in the numerical simulations and experimental data collection was a PRBS-7 pattern ($2^7 - 1$ bits, containing all possible 7-bit-long combinations of 1 s and 0 s). To improve the agreement between

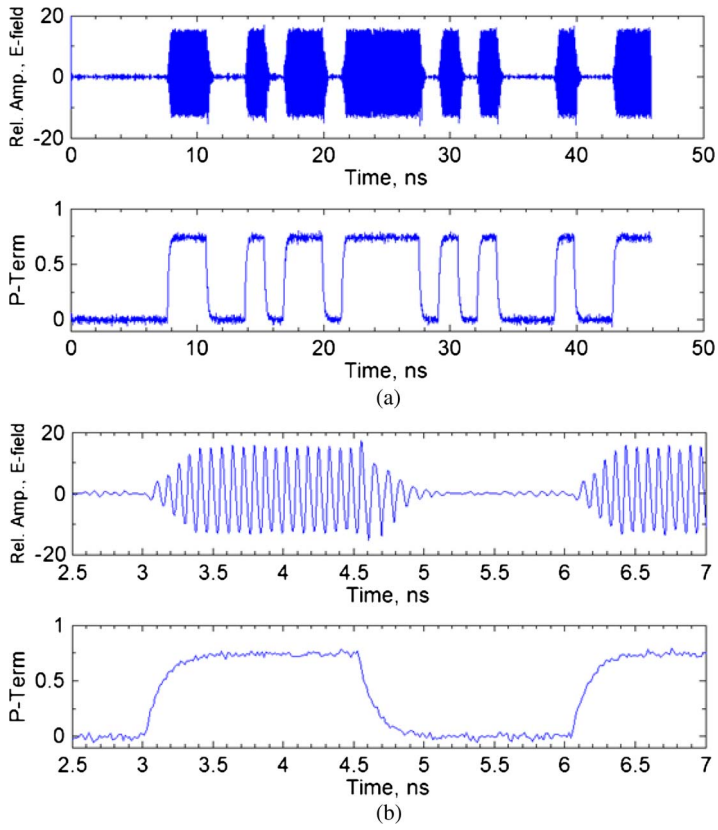

Fig. 3. (a) Simulated time response given a pseudo random bit sequence modulating the slave laser's driving current. (b) Similar results but with better temporal resolution to illustrate the mm-wave oscillations where the injected slave laser is modulated into and out of period-one operation. The modulating PRBS signal is shown below each mm-wave signal, where the bit rate is 667 Mbps.

our simulations and experiments, this modulating signal is passed through a low-pass filter to yield a signal comparable with the signal generator used in the experimental setup. Although not fully rigorous, a noise term (with a standard deviation set at 5% of the pumping term) has been added to the pumping term to more closely mirror the real-world implementation of the system, as well as to indicate the system's robustness against small perturbations. The simulation is achieved by solving (1)–(3) and unnormalizing the time constant of the result in order to enable comparison with experimental data sets. To remove the baseband component from the resultant electric-field solution, a simulated high-pass filter is utilized. In Fig. 3, $\eta_N = 0.086$ and $\Omega = 0.0$, resulting in a period-one frequency of 12.5 GHz. The values for T, P, and α were representative of the slave laser used in validating the numerical model and are summarized in Table 1.

While 12.5 GHz is not the ideal subcarrier frequency for such applications as ROF, this value was the numerical simulation goal given the experimental results. The experimental configuration, described in detail in Section 4, is comprised primarily of SubMiniature version A (SMA) components (attenuators, splitters, etc.), which limit the operational frequency range to 18 GHz. The importance of the numerical simulation results presented here is the ability to model the optically injected system while the slave laser is under direct modulation. The modulation rate of the microwave subcarrier is limited by the time necessary for the undamped relaxation oscillations of the coupled system to reach steady state. This time transient is exemplified in Fig. 3(b), whereby the period-one oscillation frequency is lower at the turn-on/off transient. Additional limitations owe to the conventional case of achieving a suitable number of microwave oscillation periods per each bit cycle. Experimentally, the electrical modulation parasitics of the semiconductor laser mount/packaging limited modulation rates to roughly 1 Gbps.

TABLE 1

Experimentally measured slave parameters at a bias current of 16 mA

Parameter	*Value*
α (linewidth enhancement factor)	3
γ_c (cavity decay rate)	333 GHz
γ_s (spontaneous carrier relaxation rate)	11.7 GHz
γ_n (differential carrier relaxation rate)	8.66 GHz
L (cavity length)	300 μm
P (normalized pumping term)	0.74
T (carrier to photon decay rate ratio)	28.5

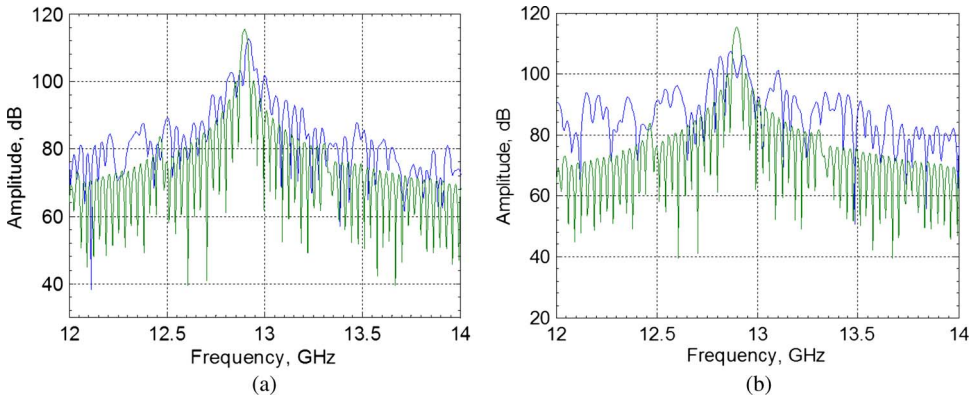

Fig. 4. (a) FFT of the mm-wave generated under optical injection with random-noise deviation 5% of *P* (blue), and without random noise (green). (b) Analogous spectra with the random noise having a 10% deviation.

The impact of the random noise applied to the simulated pumping term results in a slight noticeable shift in the amplitude of the mm-wave oscillations in Fig. 3. This impact is further highlighted in the Fourier transform of the signal (see Fig. 4) where the Fourier transform of the nonmodulated mm-wave signal with noise is compared with the Fourier transform of the signal without noise applied. The spectral purity of the signal degrades as the magnitude of the random noise is increased, qualitatively visualized by a decrease in the maximum power and additional frequency components in the noise containing spectra as shown in Fig. 4. The decrease in noise suppression, measured as the relative power difference between the peak spectral component to the next oscillatory peak (noise), is depicted in Fig. 6. Given the time-scale difference between the photon lifetime and noise fluctuations, the noise serves as a small-signal modulation as it approaches 10% of the pumping level, resulting in multiple period-one operating points. Beyond a random-noise strength of 10% (of the pump), the frequency content of the signal became highly diverse resulting in a broadened spectrum with no primary harmonic observed.

Given that the pumping current is highly stable in the laboratory environment, noise is more appropriately incorporated in the numerical model via the injection strength term η_N. The injection strength component will contain noise components due to fluctuations in the coupling mechanism between the master and slave, and any time-varying polarization changes in the injected master laser light (due to, among other things, the use of nonpolarization-maintaining fibers). For the case where random noise is added to the injection strength parameter, numerical simulations show a higher degree of stability in the mm-wave subcarrier in comparison with normalized noise levels added to the pumping term. Qualitatively, this result was not expected due to the strong correlation between the injection strength to the resonance frequency and overall damping rate of the coupled

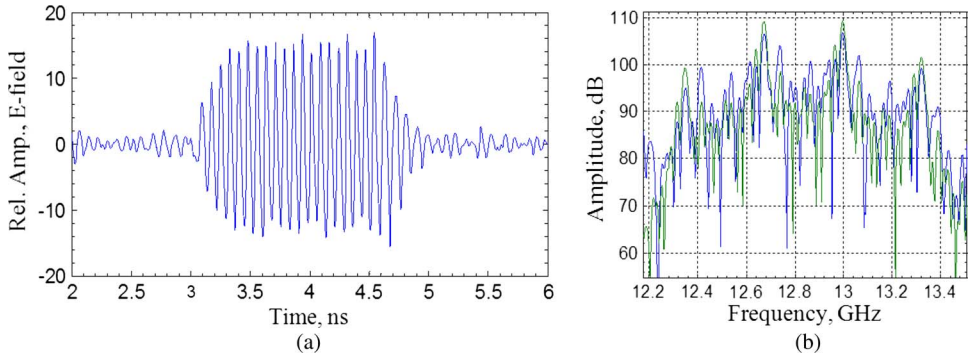

Fig. 5. (a) On–off keyed period-one mm-wave subcarrier in the presence of random noise applied to the injection strength term. The noise has a standard deviation of 10% the injection term. (b) FFT of the modulated mm-wave generated under optical injection with random noise having a 10% magnitude (blue), and without random noise (green).

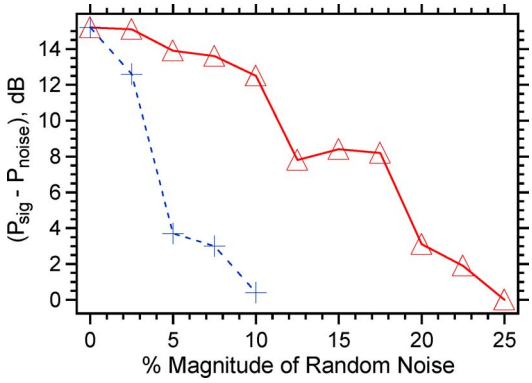

Fig. 6. Relationship between the power difference between the peak of the electrical power spectra and next strongest oscillatory peak. Blue dotted line: random noise applied to the pumping term. Red solid line: random noise applied to the injection strength term.

system [19]. With the random noise removed from the pumping term of the slave laser, random noise having a magnitude of 10% the injection strength is simulated in Fig. 5 where the slave laser's pumping term is modulated using a square-wave pattern with a 50% duty cycle. Here, the magnitude and frequency of the mm-wave subcarrier is observed to vary. The small degree of change observed in the mm-wave subcarrier shows a relative tolerance to random variations of the level investigated. The Fourier transform of the square-wave modulated signal with noise applied to the injection strength term is given in Fig. 5, whereby an increased degree of noise is observed. The primary spectral component power compared with the next strongest spectral component as a function of random-noise strength is given in Fig. 6.

4. Experimental Generation and Modulation of the mm-Wave Signal

The experimental investigation of the on–off keyed mm-wave signal was accomplished using a fiber-pigtailed quantum-well Fabry–Perot laser diode in a 5.6-mm Transmitter-the-Outline-can (TO-Can) package as the slave laser. The threshold current of the device was 11.4 mA, and the operating current was 16 mA, where the output power coupled into the fiber was 0.45 mW and the peak Fabry–Perot mode was at 1547 nm. The master laser was an external cavity tunable laser, and its wavelength was adjusted around the peak Fabry–Perot mode. The injected laser power, measured at Port 2 of the optical circulator (see Fig. 7), was held constant throughout this paper. The modulating signal, applied to a bias tee in the diode laser mount, was in the form of

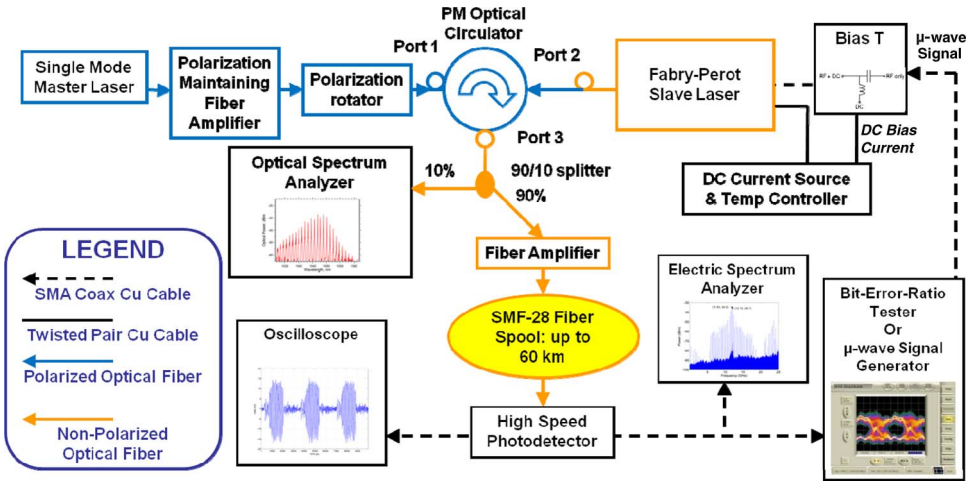

Fig. 7. Experimental setup used to validate the prediction of the single mode rate equations numerical simulations.

a 1-V P-P signal. A description of the experimental setup is given in Fig. 7. The period-one waveforms collected were unique in nature; they were not limited by the 50-GHz bandwidth oscilloscope (Agilent 86100C) nor our 25-GHz photodiode (NewFocus 1414) used in the experimental setup. Data collection was also supported by an optical spectrum analyzer with 10-pm resolution (Yokogawa AQ6317B) and an electrical spectrum analyzer with a 3-Hz–50-GHz frequency range of operation (Agilent E4448A PSA). To produce the PRBS, the slave laser was modulated using a BERT (SyntheSys Research BSA7500A).

The characterization of the injected slave laser was accomplished by least-square fitting the ringing observed in the time response of the device under free-running operation when subjected to modulation using a 50%-duty-cycle square wave. This step was taken, as opposed to fitting the modulation bandwidth response (S21) of the device, due to the relaxation-oscillation frequency of the device being higher than the electrical bandwidth of the laser diode mount and packaging. The free-running temporal response was fit using the generic in (6) and (7) describing the damped cosine nature of the ringing observed in the transient temporal photon density response to current modulation [31]. In (6), P_{out} is the measured output power of the laser, γ is the damping rate, and Ω_{osc} is the oscillation frequency defined in (7)

$$dP_{out}(t) = dP_{out}(\infty)\left[1 - e^{-\gamma t/2}\cos(\Omega_{\text{osc}}t) - \frac{\gamma}{2\Omega_{\text{osc}}}e^{-\gamma t/2}\sin(\Omega_{\text{osc}}t)\right] \tag{6}$$

$$\Omega_{\text{osc}} = \Omega_{fr}\sqrt{1 - (\gamma/(2\Omega_R))^2}. \tag{7}$$

The spontaneous carrier lifetime was then determined from these data using the approach described in [32]. The photon decay rate was assumed to be 333.3 GHz based on the facet reflectivities, internal loss, and group index. The linewidth-enhancement factor of the device was measured to be 3 using the injection-locking approach given in [30]. The characterization of the slave laser is summarized in Table 1.

Experimental results validating the theoretical simulation in Figs. 3 and 4 are given in Fig. 8, where the system exhibited a mm-wave subcarrier frequency of 9.5 GHz under optical injection. The figure also shows the damped response of the slave laser in response to the modulation signal in the absence of optical injection. In all cases, a high-pass filter with a pass-band cutoff frequency of 6.3 GHz was placed at the oscilloscope input. In the figure, the PRBS modulation signal had a bit rate of 660 Mbps. To determine the mm-wave signal frequency, the pulse was fit with a sinusoid. The resultant electrical signal showed that the modulated period-one state can be used for

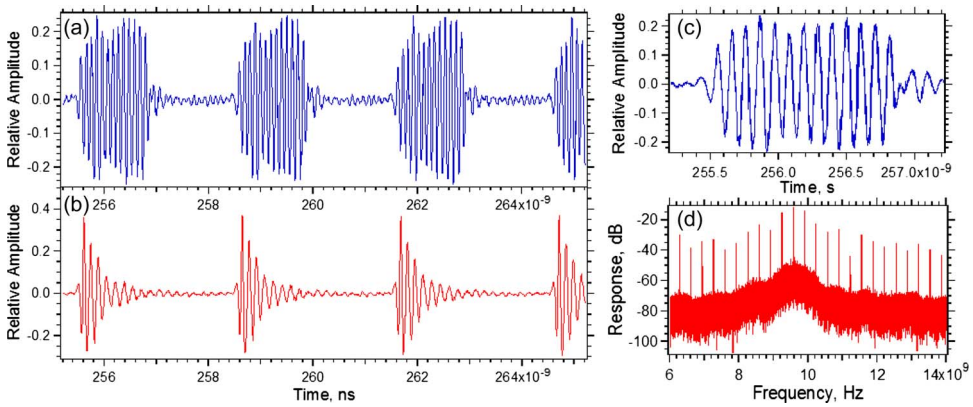

Fig. 8. Time and frequency response of the on–off keyed period-one state. In all figures the injected slave laser was modulated by a 660-Mbps square wave. (a) Signal under optical injection. (b) With the optical injection removed the slave laser experiences relaxation oscillations. (c) Close up of the mm-wave signal from (a). (d) Frequency response of the modulated period-one signal.

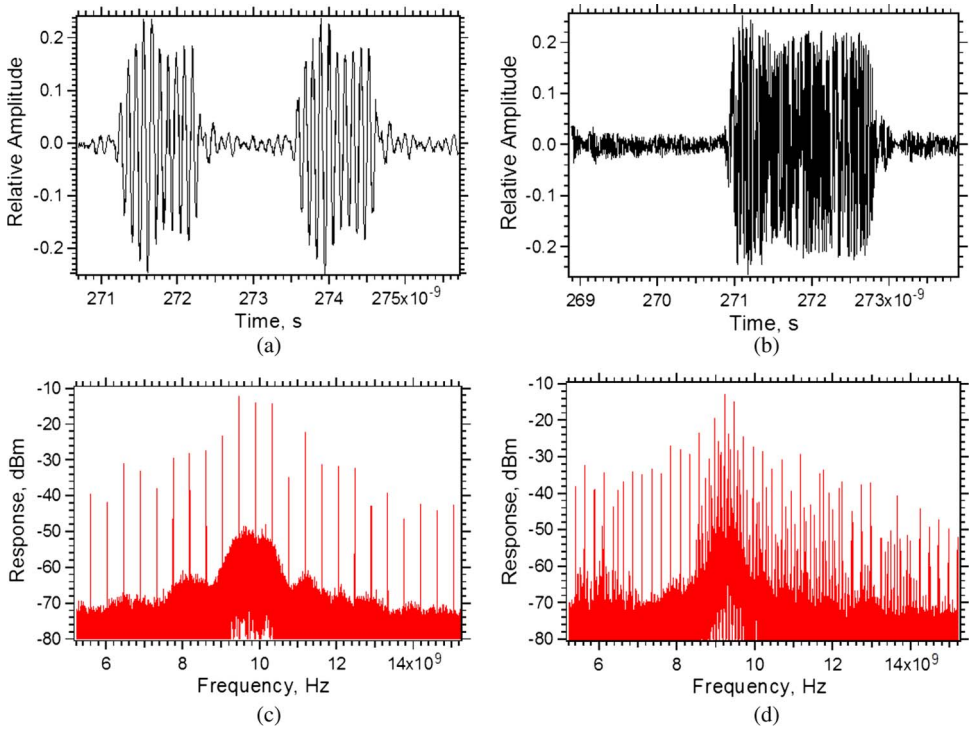

Fig. 9. (a) and (c) Stable on–off keyed mm-wave subcarrier modulated at 860 Mbps in the time (a) and frequency domain (c). (b) and (d) Unstable on–off keyed signal with a 490 Mbps modulation rate in the time (b) and frequency domain (d). The same bit sequence was used for both data rates.

transmission of both the up-converted and baseband signals given either a high-pass or low-pass filter at the output of the photodector. The instability observed in the period-one amplitude and phase is attributed to time-varying polarization changes in the injecting master laser light and/or attributed to fluctuations in the coupling between the master and slave lasers.

The modulation rate of the injected slave laser resulted in varying degrees of stability regardless of the period-one frequency generated under optical injection, as shown in Fig. 9. For each case in Fig. 9, the injection conditions were held constant, whereas the modulation rate was changed as

indicated. The initial conclusion, based on findings reported in reference [22], indicated an interaction higher order harmonics of the modulating signal reinforced the steady-state period-one oscillations. However, the experimental results discounted this relationship, leading to the understanding that stability is driven by the electrical parasitics of the laser mount and packaging.

5. Conclusion

This paper demonstrates the suitability of using the period-one state of an optically injected semiconductor laser as a mm-wave subcarrier source capable of carrying Gbps data rates. The period-one state produces a high-frequency microwave subcarrier that is easily adjustable while only requiring two dc biased semiconductor lasers. The modulation of the signal is achieve by bringing the slave laser into and out of the above-threshold lasing condition, all while under the presence of continuous wave injection from a master laser resulting in period-one operation. Given that conventional ROF approaches require an electrical modulation signal at the desired microwave subcarrier frequency and high-frequency electrical components, the optical injection approach represents a considerable simplification. Moreover, the normalized single-mode rate equation model is shown to effectively predict the time-domain behavior of the slave-laser-modulated system, along with the impact of noise on the coupled systems' stability.

Acknowledgment

The authors thank V. Kovanis for his insightful discussions. The views expressed in this article are those of the authors and do not reflect the official policy or position of the United States Air Force, Department of Defense, or the U.S. Government.

References

[1] X. Y. He, X. Fang, C. R. Liao, D. N. Wang, and J. Q. Sun, "A tunable and switchable single-longitudinal-mode dual-wavelength fiber laser with a linear cavity," *Opt. Exp.*, vol. 17, no. 24, pp. 21 773–21 781, Nov. 2009.
[2] X. Wang, W. Mao, M. Al-Mumin, S. A. Pappert, J. Hong, and G. Li, "Optical generation of microwave/millimeter-wave signals using two-section gain-coupled DFB lasers," *IEEE Photon. Technol. Lett.*, vol. 11, no. 10, pp. 1292–1294, Oct. 1999.
[3] J. O. Riely and P. Lane, "Remote delivery of video services using mm-waves and optics," *J. Lightw. Technol.*, vol. 12, no. 2, pp. 369–379, Feb. 1994.
[4] J. Yu, Z. Jia, L. Yi, Y. Su, G.-K. Chang, and T. Wang, "Optical millimeter-wave generation or up-conversion using external modulators," *IEEE Photon. Technol. Lett.*, vol. 18, no. 1, pp. 265–267, Jan. 2006.
[5] L. Chen, Y. Pi, H. Wen, and S. Wen, "All-optical mm-wave generation by using direct-modulation DFB laser and external modulator," *Microw. Opt. Technol. Lett.*, vol. 49, no. 6, pp. 1265–1267, Jun. 2007.
[6] R. T. Ramos and A. J. Seeds, "Fast heterodyne optical phase-lock loop using double quamtum well laser diodes," *Electron. Lett.*, vol. 28, no. 1, pp. 82–83, Jan. 1992.
[7] G. A. Vawter, A. Mar, V. Hietala, J. Zolper, and J. Hohimer, "All optical millimeter-wave electrical signal generation using an integrated mode-locked semiconductor ring laser and photodiode," *IEEE Photon. Technol. Lett.*, vol. 9, no. 12, pp. 1634–1636, Dec. 1997.
[8] P. Ghelfi, F. Scotti, F. Laghezza, and A. Bogoni, "Photonic generation of phase-modulated RF signals for pulse compression techniques in coherent radars," *J. Lightw. Technol.*, vol. 30, no. 11, pp. 1638–1644, Jun. 2012.
[9] L. Goldberg, H. F. Taylor, J. F. Weller, and D. M. Bloom, "Microwave signal generation with injection-locked laser diodes," *Electron. Lett.*, vol. 19, no. 13, pp. 491–493, Jun. 1983.
[10] J. Genest, M. Chamberland, P. Tremblay, and M. Tetu, "Microwave signals generated by optical heterodyne between injection-locked semiconductor lasers," *IEEE J. Quantum Electron.*, vol. 33, no. 6, pp. 989–998, Jun. 1997.
[11] S. C. Chan, S. K. Hwang, and J. M. Liu, "Period-one oscillation for photonic microwave transmission using an optically injected semiconductor laser," *Opt. Exp.*, vol. 15, no. 22, pp. 14 921–14 933, Oct. 2007.
[12] Y. S. Juan and F. Y. Lin, "Photonic generation of broadly tunable microwave signals utilizing a dual-beam optically injected semiconductor laser," *IEEE Photon. J.*, vol. 3, no. 4, pp. 644–650, Aug. 2011.
[13] A. J. Seeds and K. J. Williams, "Microwave Photonics," *J. Lightw. Technol.*, vol. 24, no. 12, pp. 4628–4641, Dec. 2006.
[14] R. C. Williamson and R. Esman, "RF Photonics," *J. Lightw. Technol.*, vol. 26, no. 9, pp. 1145–1153, May 2008.
[15] T. B. Simpson and J. M. Liu, "Enhanced modulation bandwidth in injection-locked semiconductor lasers," *IEEE Photon. Technol. Lett.*, vol. 9, no. 10, pp. 1322–1324, Oct. 1997.
[16] S. C. Chan and J. M. Liu, "Tunable narrow-linewidth photonic microwave generation using semiconductor laser dynamics," *IEEE J. Sel. Topics Quantum Electron.*, vol. 10, no. 5, pp. 1025–1032, Sep./Oct. 2002.
[17] E. K. Lau, X. Zhao, H. K. Sung, D. Parekh, C. Chang-Hasnain, and M. C. Wu, "Strong optical injection-locked semiconductor lasers demonstrating > 100-GHz resonance frequencies and 80-GHz intrinsic bandwidths," *Opt. Exp.*, vol. 16, no. 9, pp. 6609–6618, Apr. 2008.

[18] J. M. Liu, *Applications of Nonlinear Dynamics*. Berlin/Heidelberg, Germany: Springer-Verlag, 2009, pp. 341–354.
[19] M. Pochet, N. A. Naderi, Y. Li, V. Kovanis, and L. F. Lester, "Tunable photonic oscillators using optically injected quantum-dash diode lasers," *IEEE Photon. Technol. Lett.*, vol. 22, no. 11, pp. 763–765, Jun. 2010.
[20] C. Cui and S.-C. Chan, "Performance analysis on using period-one oscillation of optically injected semiconductor lasers for radio-over-fiber uplinks," *IEEE J. Quantum Electron.*, vol. 48, no. 4, pp. 490–499, Apr. 2012.
[21] S. K. Hwang, H. F. Chen, and C. Y. Lin, "All-optical frequency conversion using nonlinear dynamics of semiconductor lasers," *Opt. Lett.*, vol. 34, no. 6, pp. 812–814, May 2009.
[22] C. Cui, X. Fu, and S.-C. Chan, "Double-locked semiconductor laser for radio-over-fiber uplink transmission," *Opt. Lett.*, vol. 34, no. 24, pp. 3821–3823, Dec. 2009.
[23] M. Pochet, N. A. Naderi, V. Kovanis, and L. F. Lester, "Optically injected quantum-dash lasers at 1550 nm employed as highly tunable photonic oscillators," in *Proc. CLEO*, 2010, pp. 1–2.
[24] T. B. Simpson, J. M. Liu, A. Gavrielides, V. Kovanis, and P. M. Alsing, "Period-doubling cascades and chaos in a semiconductor laser with optical injection," *Phys. Rev. A, Atom., Mol., Opt. Phys.*, vol. 51, no. 5, pp. 4181–4185, May 1995.
[25] T. B. Simpson, "Mapping the nonlinear dynamics of a distributed feedback semiconductor laser subject to external optical injection," *Opt. Commun.*, vol. 215, no. 1-3, pp. 135–151, Jan. 2003.
[26] A. Gavrielides, V. Kovanis, and T. Erneux, "Analytical stability boundaries for a semiconductor laser subject to optical injection," *Opt. Commun.*, vol. 136, no. 3/4, pp. 253–256, Mar. 1997.
[27] T. Erneux, V. Kovanis, A. Gavrielides, and P. M. Alsing, "Mechanism for period-doubling bifurcation in a semiconductor laser subject to optical injection," *Phys. Rev. A, Atom., Mol., Opt. Phys.*, vol. 53, no. 6, pp. 4372–4380, Jun. 1996.
[28] M. Pochet, N. A. Naderi, N. Terry, V. Kovanis, and L. F. Lester, "Dynamic behavior of an injection-locked quantum-dash Fabry–Perot laser at zero-detuning," *Opt. Exp.*, vol. 17, no. 23, pp. 20 623–20 630, Nov. 2009.
[29] M. Pochet, N. A. Naderi, V. Kovanis, and L. F. Lester, "Modeling the dynamic response of an optically injected nanostructure diode laser," *IEEE J. Quantum Electron.*, vol. 47, no. 6, pp. 827–833, Jun. 2011.
[30] G. Liu, X. Jin, and S. L. Chuang, "Measurement of linewidth enhancement factor of semiconductor lasers using an injection-locking technique," *IEEE Photon. Technol. Lett.*, vol. 13, no. 5, pp. 430–432, May 2001.
[31] L. A. Coldren and S. W. Corzine, *Diode Lasers and Photonic Integrated Circuits*. New York: Wiley, 1995, pp. 204–207.
[32] N. Naderi, M. Pochet, F. Grillot, N. Terry, V. Kovanis, and L. F. Lester, "Modeling the injection-locked behavior of a quantum dash semiconductor laser," *IEEE J. Sel. Topics Quantum Electron.*, vol. 15, no. 3, pp. 563–571, May/Jun. 2009.